J. Mater. Environ. Sci. 7 (9) (2016) 3371-3380
ISSN : 2028-2508
CODEN: JMESC

Use of Silica Particles made by Nonionic Surfactant for VOCs Sorption

Oumaima Difallah and Hadj Hamaizi*

Laboratoire de Chimie des Matériaux, Faculté des Sciences Appliquées et Exactes, University of Oran 1 Ahmed Ben Bella, BP 1524 Oran, Algeria

Received 30 Dec 2015, Revised 31 Mar 2016, Accepted 11 Apr 2016
**Corresponding author. E-mail: hamaizimizou@yahoo.fr; (H. Hamaizi); Phone: +213-550-462417; fax: +213-41513077// +213-41416021*

Abstract

Adsorption of light organic compounds such acetone, 1-propanol and carbon dioxide was tested by using mesoporous silica materials made from non ionic surfactant with long chain and silica sources as tetraethylorthosilicate (TEOS) and modified Na-X Zeolite. X-ray powder diffraction (XRD), nitrogen adsorption–desorption analysis and scanning electron microscopy (SEM) were applied to characterize the silica particles of a variety prepared samples. Acetone, 1-propanol and CO_2 adsorption at 298K was evaluated by a volumetric method and indicate a high sorption capacity of organic compounds depending essentially on the porous texture of adsorbents. An adsorption kinetic model was proposed to describe the adsorption of VOCs over template-free mesoporous silica materials. A good agreement with experimental data was found.

Keywords: Amorphous materials, Sol-gel chemistry, X-ray diffraction, Adsorption.

1. Introduction

VOCs are typical gaseous emissions from various industries which pose hazards for human health and environment. Many techniques have been currently proposed for the treatment of volatile organic compounds, such as adsorption, incineration and catalytic reduction, have been developed and widely applied for VOCs removal from gaseous effluents [1,2]. The adsorption process is widely applied because the system's flexibility, simplicity, low cost and low energy consumption [3]. The main objective of this study is to investigate the adsorption properties of silica mesostructures in order to understand its usefulness as an adsorbent for important light hydrocarbons removal particularly, CO_2 (carbon dioxide), C3 (acetone and 1-propanol). Organic solvents are emitted or evaporated into the atmosphere and are the sources of about 40 Vol. % of the volatile organic compound entering the atmosphere. Their elimination from the atmosphere is a must. For this purpose, many methods have been developed such ones proposed by Caroll and Ruddy [4]. Adsorption of these contaminants onto adsorbents for purifying polluted air and subsequent desorption for eventual reuse have been the main purpose. Among these methods, adsorption is considered as the most promising technology used in organic solvent recovery and energy saving [5]. In which adsorption efficiency is governed by both adsorbate and adsorbent characteristics. Therefore, the choice of an appropriate adsorbent is very important [6]. In order to understand the nature of the adsorption process, parameters influencing it such as pore size, surface properties, pore structure and morphology of the adsorbents on VOCs uptake have been studied as reported in the literature [7,8]. However, most research projects are focused on investigating the influences of one or two kind of similar adsorbents on the VOCs adsorption. While few authors have reported the specific impact of pore structure of different kind of materials in the adsorption/desorption process. For example Kosuge et al. [9] have investigated the porous properties of various adsorbents and VOCs adsorption/desorption, just focusing on the pore structure and morphology of mesoporous silica. Therefore, nowadays most research is focused on adsorbent selection with a good stability and regeneration performance recently. Zeolites, as others kind of porous materials, are also proposed for VOCs adsorption [10-12]. Discovered in the early 90's by Kresge et al. [13] and Beck et al. [14], ordered mesoporous materials are usually obtained in the presence of surfactants which act as organic

structuring agents and molecular inorganic precursors. The interaction between organic and inorganic counter parts leads to the formation of ordered hybrid mesophases. Among the ordered mesoporous siliceous materials, there are those that are obtained from non-ionic surfactants such as di-block copolymers C_nH_{2n+1}-$(EO)_x$ called MSU-X (*Michigan Silica University*) and reported by Bagshaw et al.[15]; Huo et al.[16]; Ryoo et al.[17] and Richer and Mercier [18], and those who can reach 10 nm and 3nm in pore size and wall thickness respectively. Because these materials contain high surface areas (>700 m^2 g^{-1}), large pore volumes and large nanoscale pores. Mesoporous materials with pore sizes ranging from 2 to 50 nm have found many applications in the adsorption of gas and liquid [19]. The wormhole channel motif is a potentially important structural feature for favorable adsorption, in part, because channel branching within the framework can facilitate access to reactive sites on the framework walls. HMS (*hexagonal Mesoporous Silica*) wormhole structures, like MSU-X can also have relatively small fundamental particle sizes (<200 nm), which result in complementary textural mesoporosity for the more efficient transport of reagents to framework reaction centers as shown by Zhang et al.[20].
In this work, to further study the effect of porous textural (micro-and mesopores) on the adsorption of acetone, 1-propanol and carbon dioxide, a set of ordered spherical and disordered worm-like mesoporous silica materials have been synthesized with di-block type copolymers C_nH_{2n+1}-$(EO)_x$ as templating agents using tetraethylorthosilicate and faujasite zeolite-type as silica sources. Adsorption of VOCs is investigated at room temperature and the modified Avrami's kinetic equation was applied to determine kinetic's parameters.

2. **Experimental**

2.1. *Chemical materials*

Microporous material 13X (Na-X; CAS No. 63231-69-6) was supplied by Zeochem AG, Switzerland. Commercial zeolite was calcined in air at 823K for 6 hours to eliminate organic impurities and used as silica source. Polyoxyethylene (18) cetyl ether (C_{16}-EO_{20}) named Brij®58 and Polyoxyethylene (20) oleyl ether (C_{16}-EO_{20}) named Brij®98 has been provided by ACROS Organics Inc. Polyoxyethylene (40) nonylphenyl ether, branched ($C_{15}EO_{40}$) named IGEPAL®CO-890, Polyoxyethylene (150) dinonylphenyl ether, branched ($C_{24}EO_{150}$) named IGEPAL®DM-970, Polyethylene glycol tert-octyl phenyl ether named Triton™ X-100 and tetraethylorthosilicate (Si-$(OC_2H_5)_4$) TEOS were purchased From Aldrich-Sigma, USA. Chemical formulas of all surfactants used are given in Table 1. Deionized water and hydrochloric acid (HCl 1mol.L^{-1}) have been used for each synthesis; HCl 1mol.L^{-1} solution was prepared from 37% fuming hydrochloric acid (Aldrich-Sigma). Volatile compounds such as acetone (M = 58.08g.mol^{-1}, T_B°~ 56-57° C), 1-propanol (M = 60.10g.mol^{-1}, T_B°~ 97-98° C) purchased by Sigma-Aldrich, USA and highly pure carbon dioxide (99.99%) produced by Air Liquid, France, are used for adsorption at room temperature on sorbent materials.

Table 1: Physicochemical properties of surfactants ethers type commercialized under the designation IGEPAL® CO-890, IGEPAL®DM-970, Triton™ X-100, Brij®58 and Brij®98

Designation	Chemical formula	Molar weight/ g.mol^{-1}	HLB *
IGEPAL®DM-970	$[C_9H_{19}]_2$-C_6H_3-$(EO)_{150}$-OH	6946	19
IGEPAL® CO-890	C_9H_{19}-C_6H_4-$(OC_2H_4)_{40}$-OH	1982	17
Brij®58	$C_{16}H_{33}$-$(OC_2H_4)_{20}$-OH	~1124	15.7
Brij®98	$C_{18}H_{35}$-$(OC_2H_4)_{20}$-OH	~1149	15.3
Triton™ X-100	$C_{14}H_{21}$-$(OC_2H_4)_{10}$-OH	~625	13.5

*Hydrophilic-lyophilic balance

2.2. *Synthesis of sorbents*

Easy protocol for sorbents preparation was used in this study. It consists by mixing aqueous solution of surfactant with HCl 1mol.L^{-} solution under constant stirring (~250 rpm) for 1 hour. The TEOS was added to this mixture and left under stirring (~250 rpm) for 24 hours at room temperature. The mixture was then heated at 373K during 48 hours without stirring. After filtration the obtained solid was washed and dried at 353K. For

example, 2g of Brij®98 in 30g of demineralized water was stirred for 10minutes before adding120ml of HCl 1mol.L^{-1} solution. An amount of TEOS (9g) was added to this homogeneous mixture and kept under vigorous stirring (~400 rpm) for 24 hours. The mixture was then introduced into a sealed tube and heated at 373K for 48 hours. The resulting precipitated solid product was recovered by filtration, washed and dried. Calcinations of obtained fine white powder was carried out in a tube furnace at 823K in air; this temperature was reached with a heating rate of 10K/min and a first plateau at 373K for 1h. After the second plateau at 823K for 6 hrs, the oven was cooled down at room temperature with at the rate of about 5K/min. Zeolites are attacked with a strongly concentrated acid before adding the surfactant. For a model synthesis, 2g Brij®98 and 60mL H_2O are mixed with moderate magnetic stirring ((~250 rpm) for 10 min. 60mL of HCl 1mol. L^{-1} was added drop wise to the solution with the same stirring speed for 60 minutes. This mixture is simultaneously added to 1g Na-X Zeolite (13X) with vigorous stirring for 20 hours at room temperature. A heating treatment at 393K for 3 days, results in the formation of two distinct phases, which are filtered and dried at 373K. The stepwise calcinations in air up to 823K for 6 hours gives a fine white powder for both types of zeolites used.

2.3. *Analysis of adsorbents*

Small-angle X-ray diffraction (XRD) patterns were recorded on an Ultima-IV high resolution X-ray powder diffraction (XRD) using Cu *Kα* radiation (λ = 0.15418nm) in the 2θ range of 0.5–20˚ with a scanning rate of 0.5˚/min. The X'PERTPLUS© software enabled the counting of the spectra and the calculation of pore-pore distance by indexing the reflections. The N_2 isotherms were measured by automated apparatus ASAP 2020 (Micromeritics) at 77K. Prior to N_2 adsorption analysis; the samples were degassed at 673K under vacuum for 4 hours. The BET surface areas were calculated based on the linear part of the BET plot (P/P_0: 0.05–0.35 range). The total pore volumes were estimated according to nitrogen uptake at a relative pressure (P/P_0) of ca. 0.990. The pore size distribution and pore diameter were derived from the desorption branch of the N_2 isotherms using Barrett-Joyner-Halenda method using the Halsey equation for multilayer adsorption for all samples. Morphology and particle size of the final products were observed by using scanning electron microscopy FE-SEM (JEOL-350) operating at an acceleration voltage of 20–30 kV.

2.4. *Adsorption of VOCs*

Adsorption experiments of acetone and 1-propanol were performed by thermogravimetric technique in dynamic mode on a type of unit TGA 92 SETARAM. Analyses were performed on a sample of about 100mg of powdered material. Each analysis starts with an activation phase at 623K for one hour with a temperature rise of 5K/min under nitrogen flow. The temperature is then reduced to the working temperature of 298K. The reactive gas is introduced once the sample material is saturated and the addition of mass change is observed. The material was then regenerated at 623K under nitrogen flow. This same technique of thermogravimetry was used to determine the adsorption capacities of silica materials after a contact time of 150 min with the exhaust gas. Adsorption isotherms of CO_2 were measured on the same ASAP 2020 (Micromeritics) apparatus at 273K. Sample cell was loaded with ca. 300 mg of the sorbent. Before the sorbent was gassed out in vacuum at 673K for 4 h in order to remove any adsorbed impurities, the adsorption run was carried out using highly pure CO_2 (99.999%) in a pressure ranging from 5- 760mm Hg. Maximum amount of adsorbed CO_2 (Q_m) was determined by Langmuir equation using molecular cross-sectional area (0.17nm^2) for CO_2. We propose also, a general kinetic model to describe the adsorption of CO_2 on pure siliceous samples at 0° C. The equation of adsorption rate at the pseudo-order n purposed by Lagergren [18] can be expressed in its general form (Eq. (1)):

$$\frac{\delta q_t}{(q_e - q_t)^n} = k.dt \qquad (1)$$

Where q_e and q_t are the sorption capacity at equilibrium and at time, respectively, and k is the constant rate. This equation stems from the modified Avrami's kinetic equation which implies several steps [19]. Its linear form is deduced by integrating the equation rate (Eq. (2)):

$$(q_e - q_t)^{1-n} = {q_e}^{1-n} + k(n-1)t. \qquad (2)$$

The least squares criterion was used to determine the model parameters. To check the adequacy of the model, the coefficient of correlation R^2 between the experimental and calculated data was determined. We have also checked that the value of q_e calculated by the theoretical model fit to the experimental value obtained from the Langmuir model applied to adsorption measurements of VOCs at 298 K.

3. **Results and discussion**

XRD patterns recorded on calcined samples exhibited single broad peak in the 2θ range of 0.5-3° (Figure1), indicating a poorly ordered mesostructure lacking long-rang structural order such as observed for mesostructured solids with worm-like pores [20].

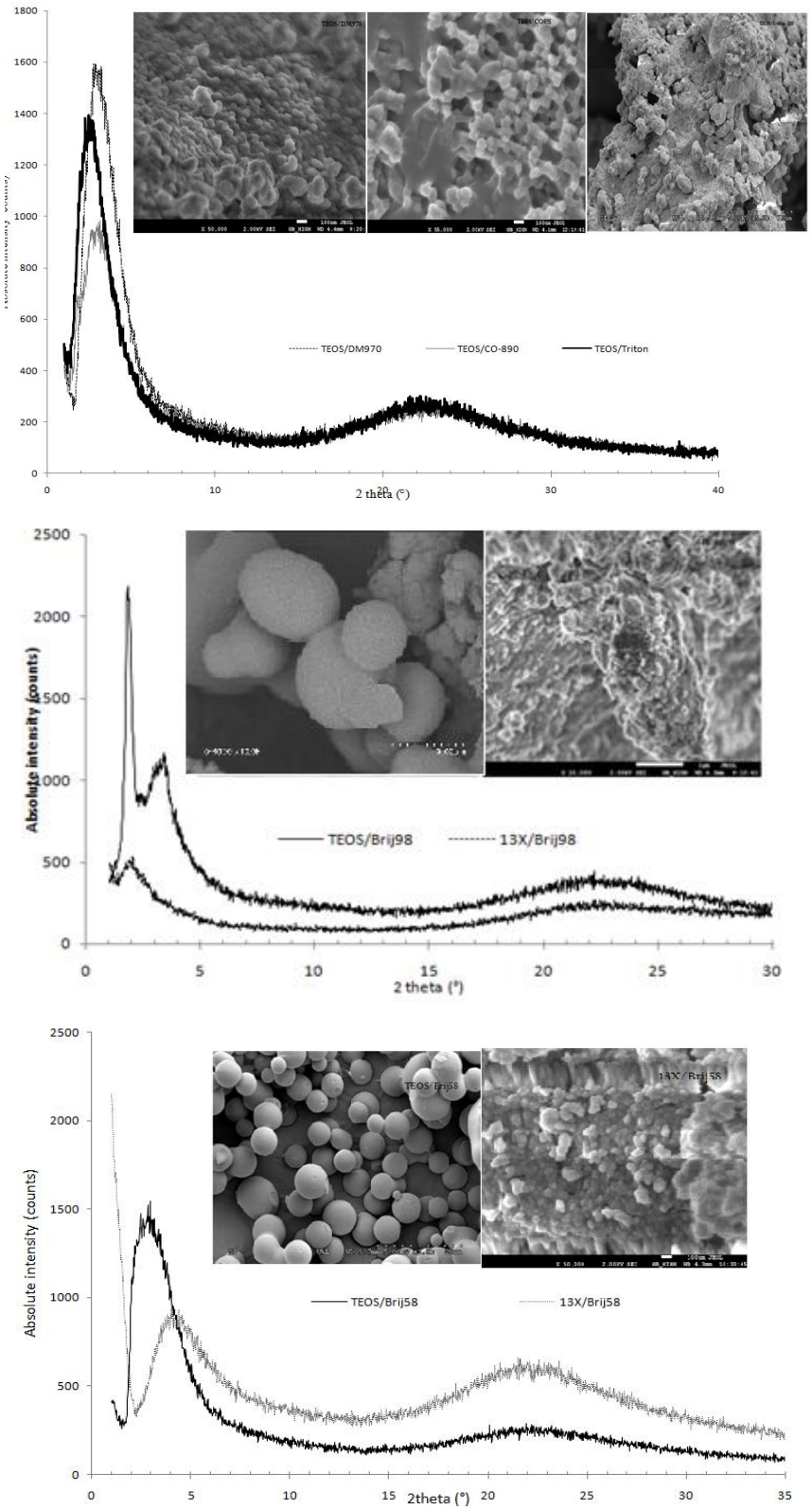

Figure 1: Low-angle XRD patterns of calcined samples. Insert: Scanning electron micrographs showing the morphology of the same samples.

According to this XRD, most of the prepared silica materials are mesotructured but with a whorm-like mesostructure and pores are regular in terms of size but not spatially ordered. For both samples denoted 13X/ Brij98 and 13X/Brij58, structure is totally modified and becomes amorphous by action of both acid and surfactant. They are characterized by the presence of a single intense reflection at 2θ=1.5-3°; it is further assumed that all the aluminum of the zeolite crystal structure was dissolved as it has been cited in many studies [21-23]. If the correlation distance deduced from the main XRD peak can be attributed to the pore-pore distance, then, the calculation gives values of 76.4Å and 56.8Å attributed for both modified zeolites, assuming respectively a cubic disposition for the two solids (Table 2). SEM observations show an entangled smalls particles ($< 1\mu m$) with pseudo cubic shape for samples TEOS/CO-890 and TEOS/DM-970 characterizes the external morphology of silica and no special morphology for Triton-X-100 otherwise an agglomerate of particles randomly arranged. Distinct spherical particles with extremely varied size ($1 - 7\mu m$) are observed for TEOS/Brij98 and TEOS/Brij58 materials. These large spheroids are a result of a high polymerization of silicate species around the micelles formed by the organic surfactant. While for modified zeolites, a very fast germination of the silicates species has led to the formation of non-uniform particles disposed in random agglomerate although for sample 13X/ Brij58 appeared thick and perpendicular layers of silica are visibly identifiable, and indicate the radical transformation of the zeolite structure with total collapse of the aluminosilicate framework. Worm-like and disordered cubic or hexagonal mesoporous textures are usually observed with such surfactants [24].

Table2. Textural and structural parameters of materials calcined at 550 °C under air for 6 hours. * used with 30g H_2O; 120 ml HCl; 9g TEOS. **used with 1g of 13X zeolite. [a]D value of characteristic reflection of calcined products. [b] Calculated at relative pressure=0.95; [c] Pore diameter calculated from desorption branch with Halsey equation; * microporous surface; ** microporous volume

Designation	Surfactant mass * (duration of synthesis at 373K)		$D_{pore-pore}$ [a] / Å	S_{BET} $m^2.g^{-1}$	Vp [b] $/cm^3.g^{-1}$	Ø [c] / Å
TEOS/DM-970	2 g DM-970	(48h)	42.4	748(57)*	0.58(0.2)**	32.2
TEOS/CO-890	2 g CO-890	(48h)	49.2	664	0.59	39.3
TEOS/Brij98	2 g Brij98	(48h)	49.2	760	0.56	39.9
TEOS/Brij58	2 g Brij58	(48h)	47.3	839	0.58	40.1
13X/Brij98	2g Brij98**	(48h)	76.4	450	0.77	71.1
13X/brij58	2g Brij58**	(48h)	56.8	366	1.16	54.1
TEOS/Triton	2 g Triton-X100	(48h)	47.5	780	0.66	47.6

Nitrogen adsorption/desorption isotherms represented for all samples in figure 2 are type IV and are characteristic for mesoporous solids; the hysteresis loop not marked and close to relative pressure value of 0.4 indicates open pores at their extremities and having dimensions of approximately 40-50 Å for samples obtained by DM-970, CO-890 and Triton-X100 respectively (Fig.2-top); It was noticed that only the TEOS/DM-970 sample has a micro porosity measured at $57m^2/g$ and $0.2cm^3/g$ for surface area and volume respectively. It would appear that the length of the hydrophilic chain of the surfactant does not necessarily lead to the formation of very large micelles and therefore very large pores considering that the surfactant molecule with a long hydrophilic chain, constituted of many ethylene oxide segments is subject of torsions resulting on size reduction before forming micelles which will have probably almost the same size from the twisted form of the surfactant molecule. Based on the physical fact that the molecule having the greatest number of oxyethylene segments generates the largest number of twists and thus forming micelles of small volume, the pore diameter can be understood that is smaller into the sample TEOS/DM-970 (32.2 Å) while it is substantially equal in other samples except for the case of TEOS/Triton X-100 (47.6 Å). For the sample 13X/Brij 98, the isotherm type IV exhibits a type H2 hysteresis, assuming open large pores (~71 Å) at their extremities while that of the other sample 13X/Brij58 is close to the type II (fig. 2-bottom). The pore size distribution in the latter sample reveals a value of 54 Å but also of 100- 220 Å that can be attributed to interparticle passages in between the silica particles. No micropores were observed in the texture proving that practically crystal lattice of the original zeolite disappeared**.**

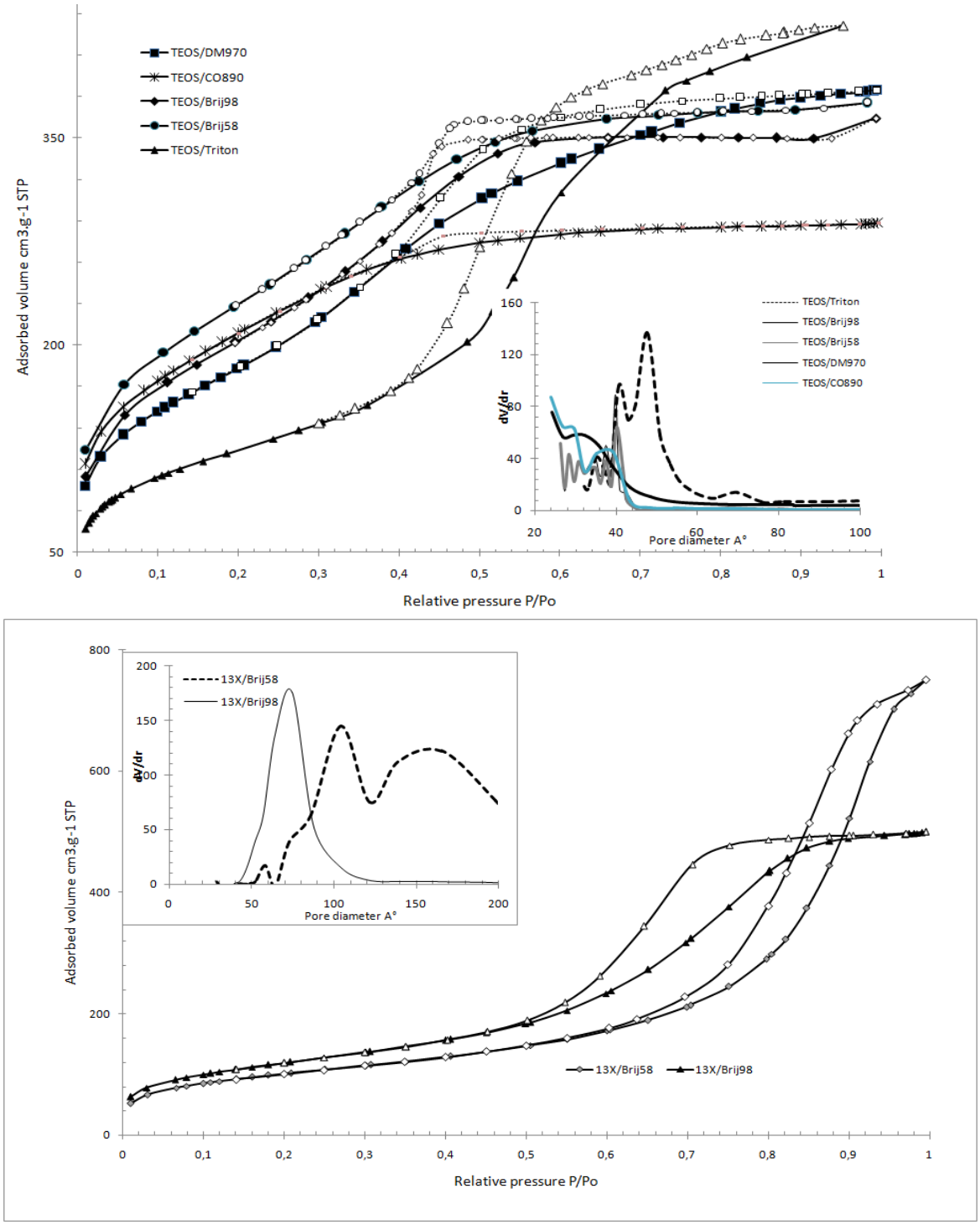

Figure 2: Nitrogen adsorption/desorption isotherms at 77 K of calcined samples. Insert: pore size distribution (PSD) obtained by BJH method applied on desorption branch.

Figure 3 shows the adsorbed quantities of acetone and 1-propanol, indicating rapid adsorption of both volatile which strongly attenuate after 40 min. onto almost all samples leading to a saturation bearing respectively ca.170mg/g and 130mg/g for acetone and alcohol. Acetone is much adsorbed in these materials as alcohol. Filling large and regular pores seems to be easier compared to a worm-like arrangement; adsorption is even better onto TEOS/CO-890 material which traps the organic molecule; the regularly increasing adsorption reached 300 and 400 mg/g respectively for acetone and 1-propanol. Furthermore, the modified zeolite adsorbs more of acetone and less of 1-propanol than the microporous 13X zeolite. The volatility of the solvent, the steric hindrance and the size of the pores explain both the difference of the adsorbed quantities.

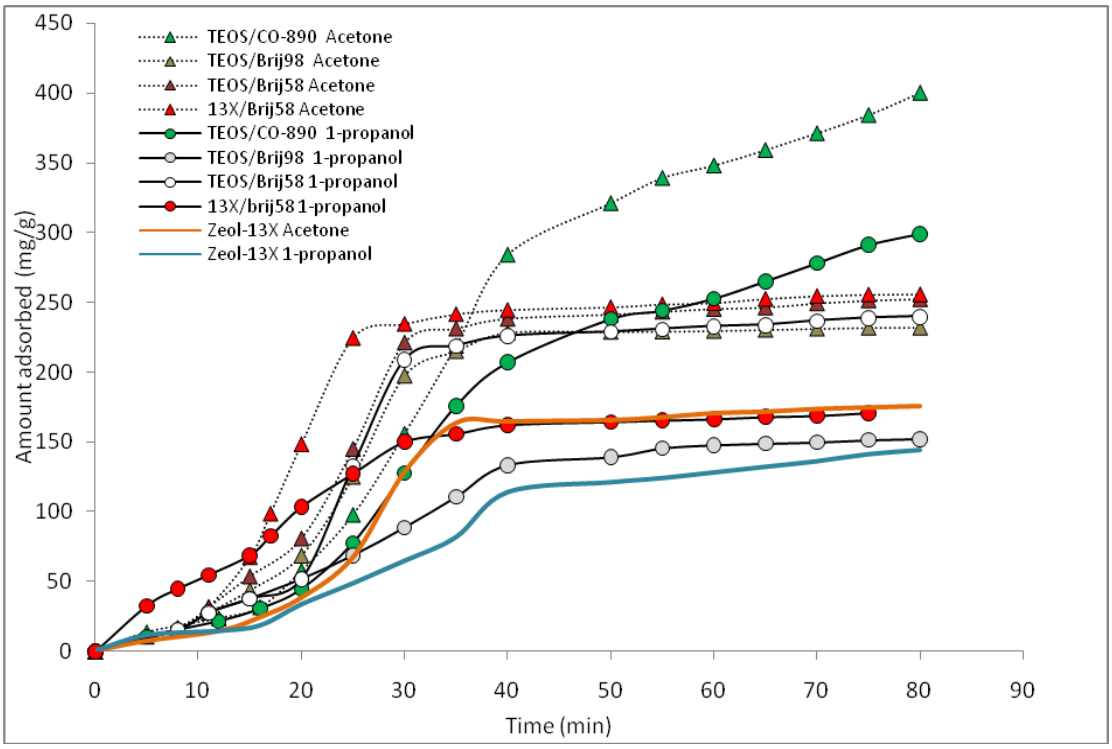

Figure 3: Adsorption breakthrough curves of acetone and 1-propanol over mesoporous silica and modified zeolite.

Figure 4 indicates the carbon dioxide adsorption breakthrough curves of different adsorbents. The equilibrium times are relatively long at the start of the experiment. Adsorption of the CO_2 molecule is carried out slowly at ambient temperature to yield, thereafter the breakthrough curves, S-shaped, with a rapid increase of adsorbed CO_2 in a minimum of time before saturation which shows very significant amounts for this purely silica mesoporous. Sample 13X/Brij98 showed a long breakthrough time compared with other porous materials, nearly 40 min.

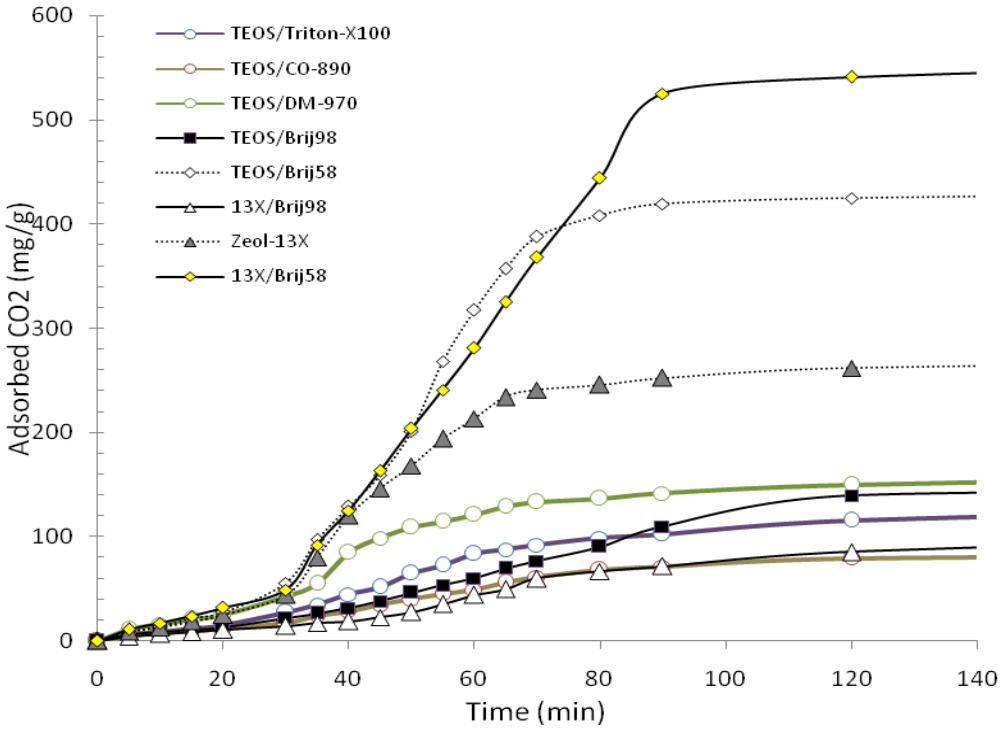

Figure 4: Adsorption breakthrough curves of CO_2 over all samples from TEOS and 13X zeolite as silica sources

The shortest breakthrough time, only 10 min. was observed on sample 13X/Brij58 and which adsorb more CO_2 than all others: ca. 540 mg/g after 100 minutes of contact time for modified 13X adsorbent unlike 13X original zeolite which adsorbs very few CO_2. It indicates that absorbents with better porous parameters (surface area and pore volume) do not necessarily show a larger breakthrough capacity. In general, the longer of the breakthrough time indicates a better dynamic adsorption capacity [25]. The modification of 13X zeolite by addition of nonionic surfactant offers very high adsorptive capacity, due to the presence of large pores generated by the interconnections of micro-mesopores better than TEOS/Brij58 sample with an exclusively mesoporous texture giving only relative low amount of adsorbed CO_2. The values of the maximum quantity adsorbed for CO_2 in this study are comparable to those reported in the literature [26-29]: Na-X (277mg/g; 162 mg/g); Na-Y (184mg/g); Na-A (211mg/g); 5A (50mg/g); HMS (74mg/g); MCM-41(29mg/g) and active carbon (396mg/g).

Table 3 shows the values of the kinetic constants and the characteristic parameters, along with the coefficient of determinations R^2 and percentage deviations Err%. The values of pseudo order kinetics n are close to 2 for the adsorption of acetone and 1-propanol in all used sorbents. The linear form of the kinetic model, which shows by extrapolation of the experimental values, a point of convergence of lines corresponding to the value fixed to $Q_e = 500mg/g$, and from which the value of the pseudo-order n is derived by calculation for acetone and 1-propanol (Figure5). Probably the lateral interactions of these both polar molecules allow a greater diffusion towards the surface and hence a more substantial adsorption.

Table3. Values of the kinetics model parameters

Sample	n	k (mg.min/g)	R^2	Q_m (mg/g)	Q_{pred} (mg/g)	Err%
Acetone						
TEOS/CO-890	1.964	$5.18\ 10^{-5}$	0.997	600	630	5.00
TEOS/Brij98	2.143	$0.08\ 10^{-5}$	0.995	450	422	6.22
13X/Brij98	1.949	$0.10\ 10^{-5}$	0.997	700	698	0.28
1-propanol						
TEOS/CO-890	1.985	$3.05\ 10^{-5}$	0.994	520	548	5.31
TEOS/Brij98	2.116	$1.34\ 10^{-5}$	0.982	300	262	12.6
Carbon dioxide						
TEOS/CO-890	1.551	$2.69\ 10^{-4}$	0.996	150	144	0.04
TEOS/DM-970	1.605	2.70 10-^{4}	0.995	310	296	0.05
TEOS/Triton	1.855	$2.30\ 10^{-4}$	0.990	250	246	0.02
TEOS/Brij98	1.648	2.19 10-^{4}	0.975	200	202	0.01
TEOS/Brij58	1.790	$2.68\ 10^{-4}$	0.981	460	465	1.07
Zeol-13X	1.661	$5.62\ 10^{-4}$	0.994	260	284	8.41
13X/Brij98	1.140	$11.8\ 10^{-4}$	0.988	120	142	15.5
13X/Brij58	1.140	$7.46\ 10^{-4}$	0.980	700	846	17.3

Whereas, in adsorption of carbon dioxide values of pseudo-order range between 1.5 and 1.8, but not for modified zeolites, where they close to 1; the quadrupole moment of CO_2 rather marked facilitates individual approach for each molecule to the solid surface. The linear form of the kinetic equation, applied to the adsorption in zeolites indicates a large gap in the straight traced between the original and modified zeolites respectively (figure6); the percentage error Q_m is therefore quite high. This suggests probably that the rates of desorption and adsorption of CO_2 molecule are equivalent in large pores open to their extremities, unlike microporous surface, wherein the adsorption rate prevails.

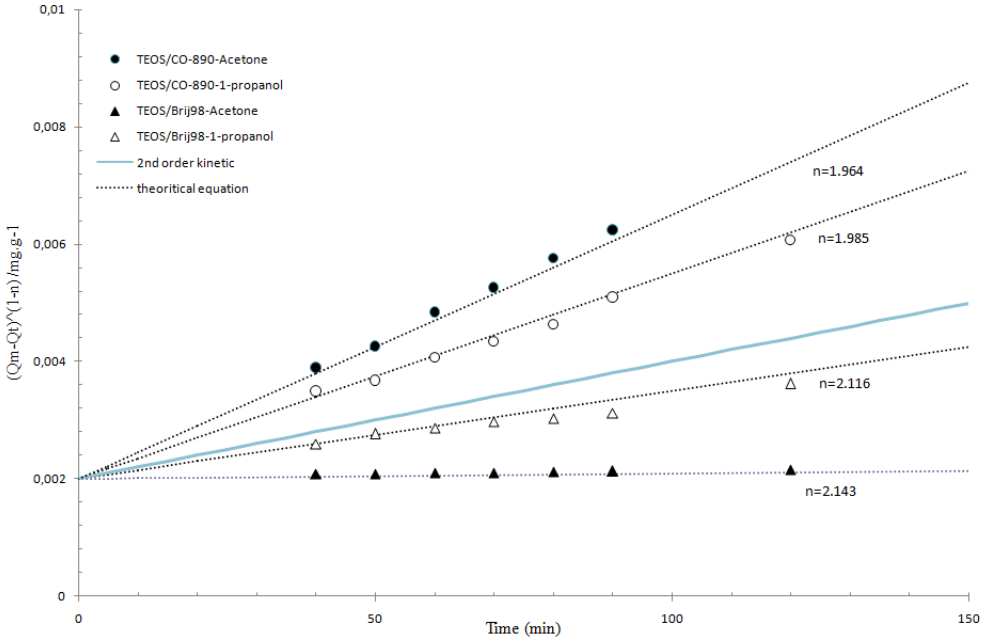

Figure 5: Acetone and 1-propanol kinetics adsorption onto purely silica at 298K (solid points: experimental; dashed lines: model)

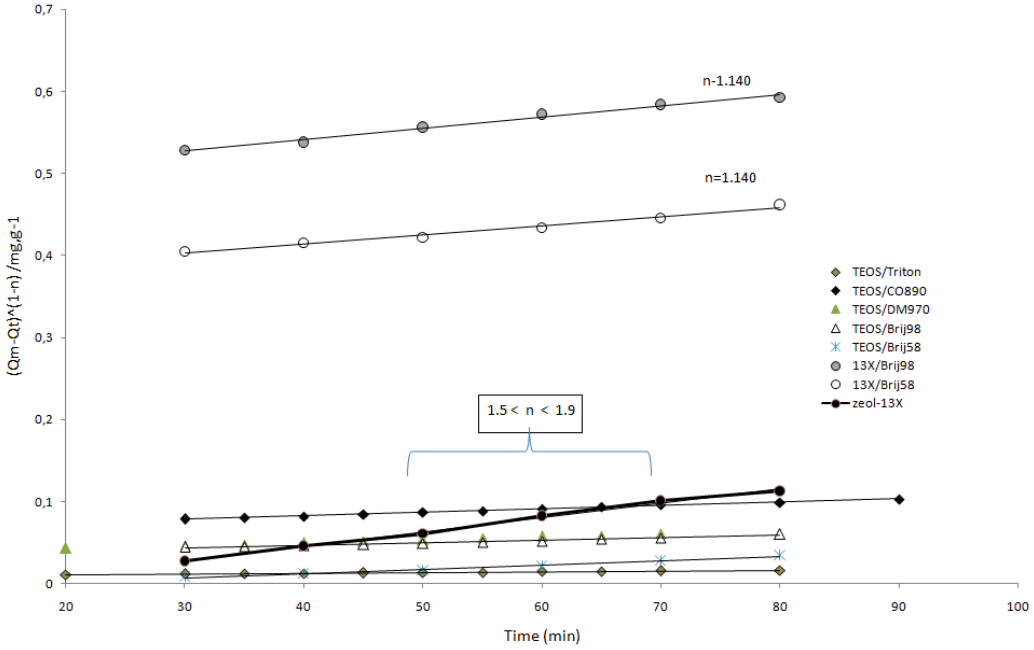

Figure 6: Carbon dioxide kinetics adsorption onto purely silica at 298K (solid points: experimental; dashed lines: model)

Otherwise, theoretical model applies very well to most kinetics models with high values of the criterion R^2, constant rate in the modified zeolites and pseudo-order for the case of light organic molecules that adsorb well in the studied

Conclusions

Mesoporous silica particles were synthesized by using non-ionic surfactants long chain as template, tetraethylorthosilicate and 13X zeolite as silica precursors. Textural characterization shows a high specific surface and large pores for samples, especially for those obtained with modified 13X zeolite, which are characterized by a high mesoporisity. Samples exhibit a better acetone, 1-propanol and CO_2 adsorption at 298K.

It is understood that the adsorbed amounts depend not only on parameters textural adsorbents but also the configuration and the polarizability of each organic molecule investigated. The lateral interactions between molecules seem to favor their adsorption as in CO_2 adsorption.This study presents a kinetic analysis of organic compounds adsorption and the proposed model was in good agreement with experimental data.

Acknowledgment(s)-This work is part of research project CNEPRU (Oran University) of the Ministry of Higher Education which has provided us with financial support; the financial support of the General Directorate of Scientific Research and Technological Development (DGRSDT). The University of Almeria is gratefully acknowledged for characterization analyzes reported in this work.

References

1. Ruddy E.N., Carroll L.A., *Chem. Eng. Prog. In Water Envir. Res.* 89 (1993) 28.
2. Braeuer, P., Salem, M., Harting, P., Quitzsch, K., *Sep. Purif. Technol*. 12 (1997) 255.
3. Khan F.K., Ghosal A.K., *J. Loss Prevention Proc. Ind.* 13 (2000) 527.
4. Guillemot M., Mijoin J., Mignard S., & Magnoux P., *Ind. Eng. Chem. Res.* 46 (13), (2007) 4614.
5. Serrano D.P., Calleja G., Botas J.A., Gutierrez F.J., *Ind. Eng. Chem. Res.*43:22 (2004) 7010.
6. Hu Q., Li J.J., Hao Z.P., Li L.D., Qiao S.Z., *Chem. Eng. J.* 149 (2009) 281.
7. Kosuge K., Kubo S., Kikukawa N., Takemori M., *Langmuir* 23 (2007) 3095.
8. Piwonski I., Zajac J., Jones D.J., Roziere J., Partyka S., Plaza S., *Langmuir* 16 (2000) 9488.
9. Tong W.Y., Kong D.J., Liu Z.C., Guo Y.L., Fang D.Y., *Chin. J. Catal.* 29 (2008) 1247.
10. Wang J., Xu F., Xie W.J, Mei Z.J., Zhang Q.Z., Cai J., *J. Hazard. Mater.* 163 (2009) 538.
11. Kresge C.T., Leonowicz M.E., Roth W.J., Vartuli J.C., Beck J.S, *Nature* 359 (1992) 710.
12. Beck J.S., Vartuli J.C., Roth W.J., Leonowicz M.E., Kresge C.T., Schmitt K.D., Chu C.T-W., Olson D.H., Sheppard E.W., McMullen S.B., Higgins J.B., Schlenker J.L., *J. Am. Chem. Soc*. 114 (1992) 10834.
13. Ryoo R., Kim J.M., Shin H.J., Lee J.Y., *Stud. Surf. Sci. Catal*. 105 (1997) 45.
14. Bagshaw S.A., Prouzet E., Pinnavaia T.J.,*Science* 269 (1995) 1242.
15. Huo Q., Margolese D., & Stucky G.D., *Chem. Mater*. 8 (1996) 1147.
16. Richer R., Mercier L., *Chem. Mater*. 13 (2001) 2999.
17. Zhang W., Pauly T.R., Pinnavaia T.J., *Chem. Mater*. 9 (1997) 2491.
18. Lagergren S, Kunglika Svenska. *Vetens. Akadem. Handligar*; 24:1 (1898)
19. Lopes E.C.N. , Dos Anjos F.S.C., Vieira E.F.S., Cestari A.R., *J. Colloid. Interface Sci*. 263 (2003) 542.
20. Pauly T.R., Pinnavaia T.J., *Chem. Mater*. 13: 9 (2001) 987.
21. Tao Y., Kanoha H., Hanzawa Y., Kaneko K., *Colloids. Surf. A: Physicochem. Eng. Aspects* 241 (2004) 75.
22. Baran R., Millot Y., Onfroy, T., Krafft J-M., Dzwigaj S., *Microporous Mesoporous Mater.* 163 (2012) 122.
23. Goto Y., Fukushima Y., Ratu P., Imada Y., Kubota Y., Sugi Y., Ogura M., *J. Porous Mater.* 9 (2002) 43.
24. Kim S. Su, Pauly T.R., Pinnavaia T.J., *Chem. Comm.* 835 (2000) 835.
25. Zhang W., Qu Z., Li X., Wang Y., Ma D., Wu J., *J. Environ. Sci.* 24 (2012) 520.
26. Fripiat J.J., Cruz M.L., Bohor B.F., Thomas J., *Clays Clay Miner.* 22 (1974) 23.
27. Lee K.B., Beaver M.G., Caram H.S., Sircar S., *Adsorption* 13 (2007) 385.
28. Chew T.L., Ahmad A.L., Bhatia S., *Adv. Colloid and Interface Sci.* 153 (2010) 43.
29. Hwang K.S., Han L., Park D.W., Oh K.J., Kim S.S., Park S.W., *Korean J. Chem. Eng.* 27 (2010) 241.